

# Quantifying the influence of land-use and surface characteristics on spatial variability in the urban heat island

Melissa A. Hart · David J. Sailor

Received: 5 July 2007 / Accepted: 30 January 2008 / Published online: 7 May 2008  
© Springer-Verlag 2008

**Abstract** The urban thermal environment varies not only from its rural surroundings but also within the urban area due to intra-urban differences in land-use and surface characteristics. Understanding the causes of this intra-urban variability is a first step in improving urban planning and development. Toward this end, a method for quantifying causes of spatial variability in the urban heat island has been developed. This paper presents the method as applied to a specific test case of Portland, Oregon. Vehicle temperature traverses were used to determine spatial differences in summertime  $\sim 2$  m air temperature across the metropolitan area in the afternoon. A tree-structured regression model was used to quantify the land-use and surface characteristics that have the greatest influence on daytime UHI intensity. The most important urban characteristic separating warmer from cooler regions of the Portland metropolitan area was canopy cover. Roadway area density was also an important determinant of local UHI magnitudes. Specifically, the air above major arterial roads was found to be warmer on weekdays than weekends, possibly due to increased anthropogenic activity from the vehicle sector on weekdays. In general, warmer regions of the city were associated with industrial and commercial land-use. The downtown core, whilst warmer than the rural surroundings, was not the warmest part of the Portland metropolitan

area. This is thought to be due in large part to local shading effects in the urban canyons.

## 1 Introduction

Land-use modifications due to urbanization can modify the energy balance in cities; this in turn affects the urban thermal environment, resulting in the urban heat island (UHI) effect, whereby urban areas often experience different temperatures than surrounding rural areas. An urban heat island can have human health and thermal comfort consequences (Voogt 2002; Huang et al. 2005), alter the city's photochemistry and affect urban air pollution (Saitoh et al. 1996; Taha 1996; Sarrat et al. 2006), initiate or affect the formation of convective storms (Jauregui and Romales 1996; Bornstein and Lin 2000), and affect the energy consumption needs of a city through impacts on heating and cooling requirements (Akbari et al. 2001; Assimakopoulos et al. 2007; Kolokotroni et al. 2007).

Changes in the thermal environment due to urbanization are influenced by many factors. Land-use and surface characteristics that can influence the urban heat island include: building density and building height to width ratio, roads and traffic density, building and surface materials whose thermal properties differ from the surrounding rural environment, the use of green space, and sky view factor (Bottyan and Unger 2003; Stone and Norman 2006; Unger 2006). A city's canyon geometry, building density and the materials used can absorb and store more incoming solar radiation due to a reduction in surface albedo or conversely store less energy due to shading (Roth 2002; Chudnovsky et al. 2004). Canyon geometry causes the city surface to emit less long-wave radiation due to reduced sky-view factor (Unger 2004; Erell and Williamson 2007). Urban

---

M. A. Hart (✉)  
Department of Geography, The University of Hong Kong,  
Pokfulam Rd.,  
Hong Kong SAR, China  
e-mail: mhart@hkucc.hku.hk

D. J. Sailor  
Department of Mechanical and Materials Engineering,  
Portland State University,  
P.O. Box 751, Portland, OR 97207, USA

surface characteristics can result in a reduction in evapotranspiration due to lack of vegetation and surface moisture (Akbari et al. 2001; Wong and Yu 2005; Jusuf et al. 2007). Urban areas are also sources of waste heat emissions due to anthropogenic activity (Sailor and Lu 2004).

Urban areas are not homogenous in their land-use and surface characteristics and the urban thermal environment not only varies from its rural surroundings but also varies within the urban area. An investigation into the spatial variability of UHI intensity in the city of Tel Aviv (Saaroni et al. 2000) found both positive and negative heat island pockets during the daytime within the city center. Warmer areas were associated with high building densities, heavy traffic flows, daytime heat sources and low sea-breeze ventilation. Cooler areas of the city were found in open regions such as plazas. The authors hypothesise that in Tel Aviv, the sea breeze is important in dictating the spatial variability of the UHI intensity as the open, cooler areas were more likely to be affected by sea-breeze penetration. An analysis of fixed and mobile measurements in the city of Gaborone, Botswana found intra-urban temperature differences were in the same range as the urban-rural differences (Jonsson 2004). In this hot, semi-arid city, vegetation was found to be the most important factor affecting the spatial variability of the daytime UHI with areas of the city containing irrigated gardens cooler than both unvegetated urban areas and the drier vegetation in the rural surroundings. In Singapore the higher UHI intensities in a commercial area compared to the CBD have been attributed to enhanced anthropogenic heat due to extended working hours in the commercial district, differences in green space and distance to water bodies (Chow and Roth 2006). An investigation of the impact of different land-use variables on UHI intensity at three different housing estates within Hong Kong, found UHI intensity varied up to 1.5°C during the daytime (Giridharan et al. 2004) and 1.3°C at night (Giridharan et al. 2005) within the estates. The most important land-use factors found to influence UHI intensity were albedo, sky-view factor, height to total floor area ratio and altitude. A more recent study by Giridharan et al. (2007) extended their study both spatially and temporally and found that seasonal differences were more influential on UHI than geographical characteristics. The greatest correlation between urban land use parameters and UHI intensity was found on clear days and nights during the summer.

The above examples illustrate that the urban characteristics most important to spatial variability of UHI intensity differ depending upon city morphology, location and climatic zone. Research campaigns examining the influence of urbanization on a city's climate have been taking place for many years, e.g. the Metropolitan Meteorological Experiment (METROMEX) in St Louis in the 1970s (Changnon Jr et al. 1971), and comprehensive reviews of

urban heat island research can be found in Arnfield (2003), (2006) and Souch and Grimmond (2006).

Whilst the general causes of the urban heat island are well known, it is not well understood how much influence different urbanization characteristics (e.g. land-use, road density, vegetation coverage) have on the intensity of the UHI. This paper investigates the influence of urbanization on the urban climate, and in turn assesses the causes of spatial variability in the summertime urban heat island by using a combination of mobile vehicle temperature traverses and GIS resources. A tree-structured regression model is used to quantify the land-use and surface characteristics that have the greatest influence on UHI intensity and this model is used to produce maps of summertime daytime (both weekday and weekend) UHI intensity. Portland, Oregon is used as the test case for the application of this method. While Portland is not widely viewed as a city with significant heat issues, it presents an opportunity to study a potentially vulnerable city where future population growth, expansion of the air-conditioning market, and global climate change may combine to increase the importance of the summertime UHI.

## 2 Methods and data

### 2.1 Study area

The city of Portland is the largest city in the state of Oregon with a greater metropolitan population just under 2 million. As shown in Fig. 1, Portland is located in the Pacific Northwest region of the USA at latitude of approximately 45°N. It is approximately 90 km inland from the Pacific Ocean and is in a valley bordered by a range of coastal mountains 50 km to the west and the more prominent Cascade mountain range 50 km to the east. The Willamette River runs approximately N–S through the middle of the metropolitan region and the Columbia River provides a northern border. Portland experiences a temperate climate with warm dry summers and cool wet winters (Köppen classification Csb). For the purposes of this paper, the summertime UHI is investigated for Portland. The only previous investigation of the Portland UHI was undertaken by George and Becker (2003). Their investigation of the spatial variability of the Portland UHI was undertaken as part of an undergraduate collaborative research project at Portland State University and found temperature differences across the Portland metropolitan area of up to 10°C (temperature measurements were taken just prior to sunrise on a November morning) and a decrease in UHI magnitude as a function of distance from the city center. All Oregon cities have an urban growth boundary (UGB) (Portland Metro 2002) which protects surrounding rural areas from



**Fig. 1** Location map showing the Portland metropolitan area, Willamette and Columbia Rivers and the Spangler Road rural meteorological site

being encroached on by urban sprawl and thus creates a clear divide between urban and rural areas. Every 5 years, a review of land supply is conducted and, if necessary, the UGB is expanded. The current Portland UGB encompasses 950 km<sup>2</sup>.

## 2.2 Vehicle temperature traverses

To measure the spatial variability of summertime near-surface air temperature experienced across the Portland metropolitan area vehicle traverses were undertaken on 6 days during the summer of 2006. Figure 2 shows the coverage of the Portland urban area achieved by the mobile temperature traverses with traverse traces overlain on aerial photographs. This figure shows that the vehicle traverses

covered a large amount of the Portland metropolitan area providing spatially dispersed temperature measurements.

Each traverse platform consisted of a class A ceramic wound resistance temperature detector (RTD) mounted within a 12 cm long, 2.5 cm diameter white plastic shade tube. The shade tube was supported on a passenger-side window-mounted mast approximately 25 cm above the vehicle roof and 30 cm away from the edge of the vehicle. The RTD sensors were connected to data logging temperature recorders with an estimated system accuracy of  $\pm 0.15^{\circ}\text{C}$  and a (90%) response time of less than 9 s in 1 m/s airflow; the response time for speeds the vehicles were traveling during traverses was calculated to be less than 4 s. The vehicles traveled at an average 36 km/h and the movement of the vehicle aspirated the sensors and measurements recorded when the car was



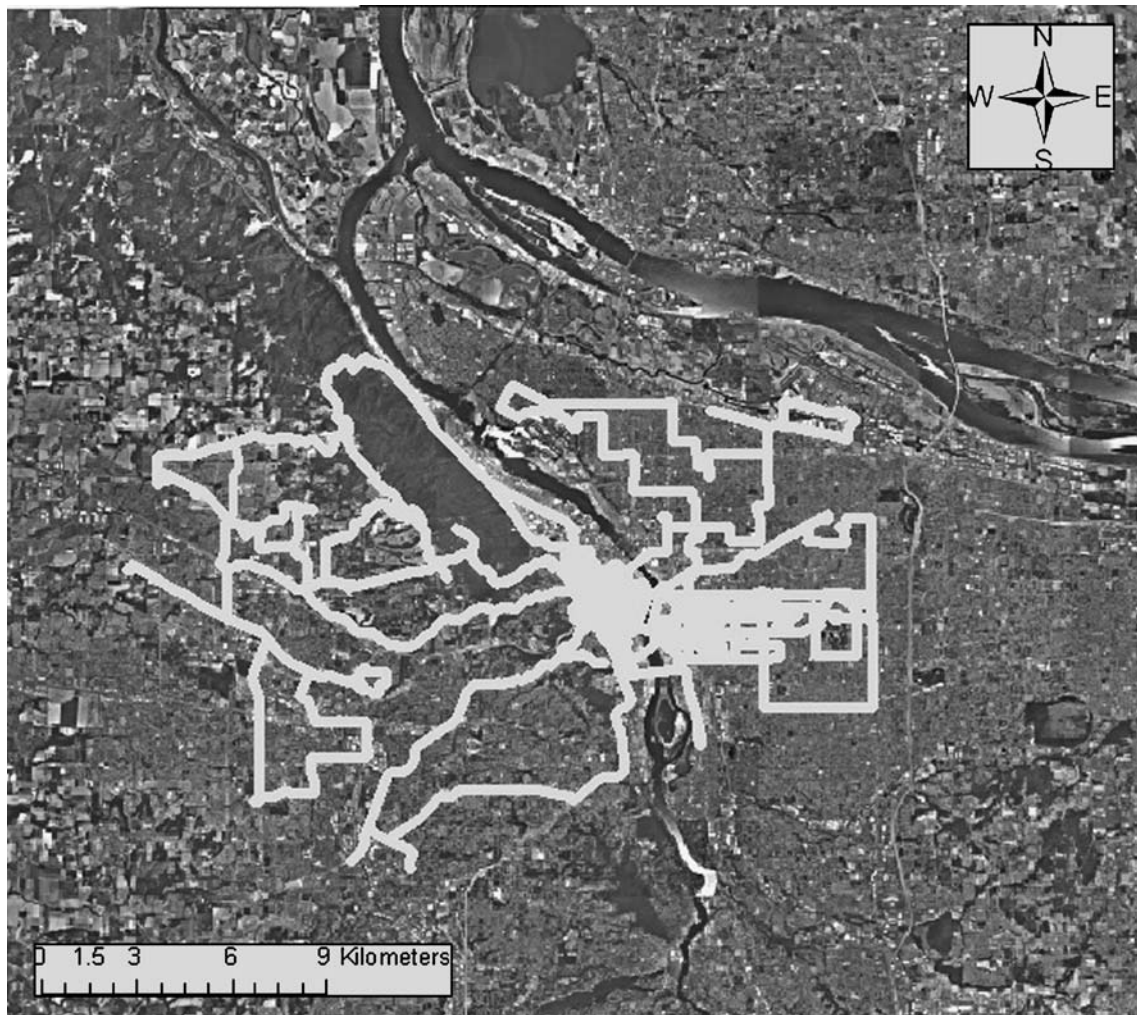


**Fig. 2** Coverage of the summer 2006 vehicle temperature traverses across the Portland metropolitan area

stationary (e.g. at traffic lights) were not used in the analysis. Temperature was recorded every 2 s. A time synchronous GPS system (BlueGPS units from RoyalTek) was also attached to each car so that each temperature measurement could be paired with a GPS location, velocity, and altitude. Each day's traverse involved between one and four cars, and lasted less than 1 h.

Elevation in the Portland area ranges from 0–330 m. Therefore temperatures were modified to correspond to the same elevation (0 m) using measured temperature lapse rates. These lapse rates were obtained from the concurrent radio-sonde accents at Salem airport, the closest measurement of the atmospheric boundary layer. Radio-sonde accents at Salem airport are undertaken in the mid afternoon (in addition to early morning), the same time period as the temperature traverses. The traverses were undertaken close to the warmest time of the day when peaks in energy consumption on summer days due to space cooling demands are experienced.

Table 1 presents the maximum and minimum temperatures on each of the traverse days in addition to the

average maximum and minimum temperatures for Portland during the summer months. All traverses were undertaken on days when the maximum temperature was significantly warmer than average maximum temperatures for that month, wind speeds were light to moderate, ranging from 3.6 to 6.7 m/s. Skies were clear for all traverses.

The difference between the measured urban temperature and a representative fixed rural site was calculated in order to determine instantaneous UHI intensity. The rural site, Spangler Road, is a pollution/meteorology monitoring site operated by the Oregon Department of Environment Quality (DEQ) located 30 km south southeast of the Portland city center (Fig. 1). A polynomial was fit to the rural site's (10 min) temperature data in order to interpolate between readings.

### 2.3 GIS resources

GIS resources were used to investigate the influence of surrounding surface and land-use characteristics on the spatial variability of the UHI. Land-use parameters used included the

**Table 1** Meteorological conditions during summer 2006 traverses

Date	Weekday (WD)/ weekend (WE)	Daily max. temp. (ave. max. for month) (°C)	Daily min. temp. (ave. min. for month) (°C)	Ave. wind speed during traverse (m/s)
26 June 2006	WD	37.8 (23.0)	18.9 (12.0)	5.6
21 July 2006	WD	40.0 (26.0)	17.8 (14.0)	6.7
22 July 2006	WE	32.2 (26.0)	23.8 (14.0)	4.1
23 July 2006	WE	37.8 (26.0)	21.1 (14.0)	3.6
24 July 2006	WD	36.1 (26.0)	22.2 (14.0)	3.6
2 September 2006	WE	34.4 (26.0)	15.0 (14.0)	4.1

proportion of land-use that was residential (single family or multi-family), commercial or industrial, the total floor space of buildings and the total length of roads. Surface characteristics included the proportion of the surface that was tree canopy, ground vegetation, impervious or loose surface cover.

#### 2.4 Surface cover

Coverage of surface characteristics was acquired from the City of Portland, Bureau of Planning (City of Portland 2006). Aerial imagery was collected using a GeoScanner system, which includes digital cameras fitted with optical filters that collect imagery in four spectral bands (visible blue, visible green, visible red, and near-infrared). Images were collected between 1 to 20 June 2002, allowing for the capture of summertime canopy cover. The images were collected at an elevation of 8,000 feet above ground, achieving a pixel resolution of approximately 1 m. Original images were converted to a single normalized difference vegetation index (NDVI) and surfaces were ultimately classified as non-canopy vegetation (i.e. grasses and shrubs), tree-canopy vegetation, loose surface, impervious surface and water. An accuracy assessment on 30 points throughout the image area indicated that the horizontal accuracy of the final georeferenced imagery averaged  $\pm 3.5$  m (City of Portland 2006).

#### 2.5 Land-use

GIS land-use information was obtained from the Portland Metro Regional Land Information System (RLIS 2006). RLIS provides spatial information of land-use in Portland at the individual land-parcel scale and information available for each land parcel includes: the total area of the land parcel, building floor space, land-use zoning of the land parcel, e.g. residential, commercial, industrial etc. In addition RLIS provides information on roads across the Portland metropolitan area.

#### 2.6 Linking temperature traverses with land-use and surface characteristics

The Portland metropolitan area was divided into an  $80 \times 55$  grid, with grid cells of 300 m. This grid was then used to

aggregate land-use and surface characteristics from the GIS resources. For each 300 m grid cell the land surface characteristics listed below (along with their possible influence on the urban energy balance) were calculated:

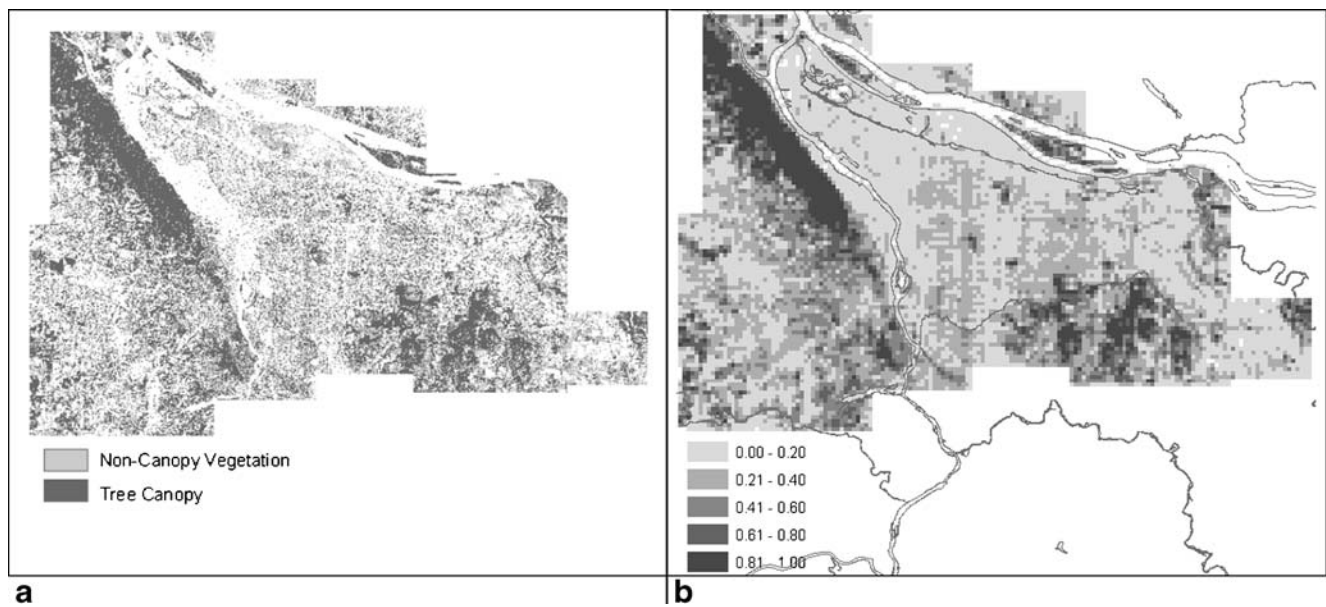
- Percentage of canopy cover: influences albedo and emissivity, absorption and storage of incoming solar radiation, emittance of long-wave radiation, moisture availability and runoff, evapotranspiration and turbulent exchanges
- Percentage of ground vegetation cover: influences albedo and emissivity, moisture availability and runoff and evapotranspiration
- Percentage of impervious surface: influences albedo and emissivity, moisture availability and runoff
- Percentage of loose surface: influences albedo and emissivity, moisture availability and runoff

Figure 3 shows the original vegetation raster, and an example of a surface characteristic aggregated to a 300-m grid. This figure illustrates the proportion of surface that is covered in tree canopy for each grid cell. The highly forested, Forest Park can be clearly seen, as can the relative scarcity of tree canopy cover in the downtown area. In addition, for each 300 m grid cell the following land-use characteristics were calculated:

- Percentage of land that was single family residential, multifamily residential, commercial or industrial: influences anthropogenic heat emissions
- Total building floor space: influences canyon geometry which in turn influences: albedo and emissivity, turbulent exchange, sensible heat storage, absorption and storage of incoming solar radiation and emittance of long-wave radiation, moisture availability and runoff, and anthropogenic heat emissions
- Total length of roads: influences anthropogenic heat emissions, albedo and emissivity, moisture availability and runoff

An example of this aggregation of land-use characteristics to a 300-m grid is shown in Fig. 4 which shows the land-use map for Portland with commercial land-use shown





**Fig. 3** **a** Raster image of non-canopy and tree canopy vegetation cover over Portland (1 m resolution), **b** the proportion of tree canopy cover in a 300 m grid cell, aggregated from the raster image

in pink and the total area of commercial land-use in each 300 m grid cell, where the more densely commercial areas are the downtown area and along the major arterial roads.

### 2.7 Regression tree analysis

To determine the importance of the various land-use and surface parameters on the spatial distribution of the urban

heat island across Portland, the statistical program CUBIST (Rulequest 2006) was used to construct a tree-structured regression model. CUBIST produces rules-based predictive models where the final model tree consists of a series of if/then (classification) rules. The dependent variable in the analysis was mean UHI intensity for each grid cell covered by temperature traverse. The independent variables in the model were the surface and land-use characteristics

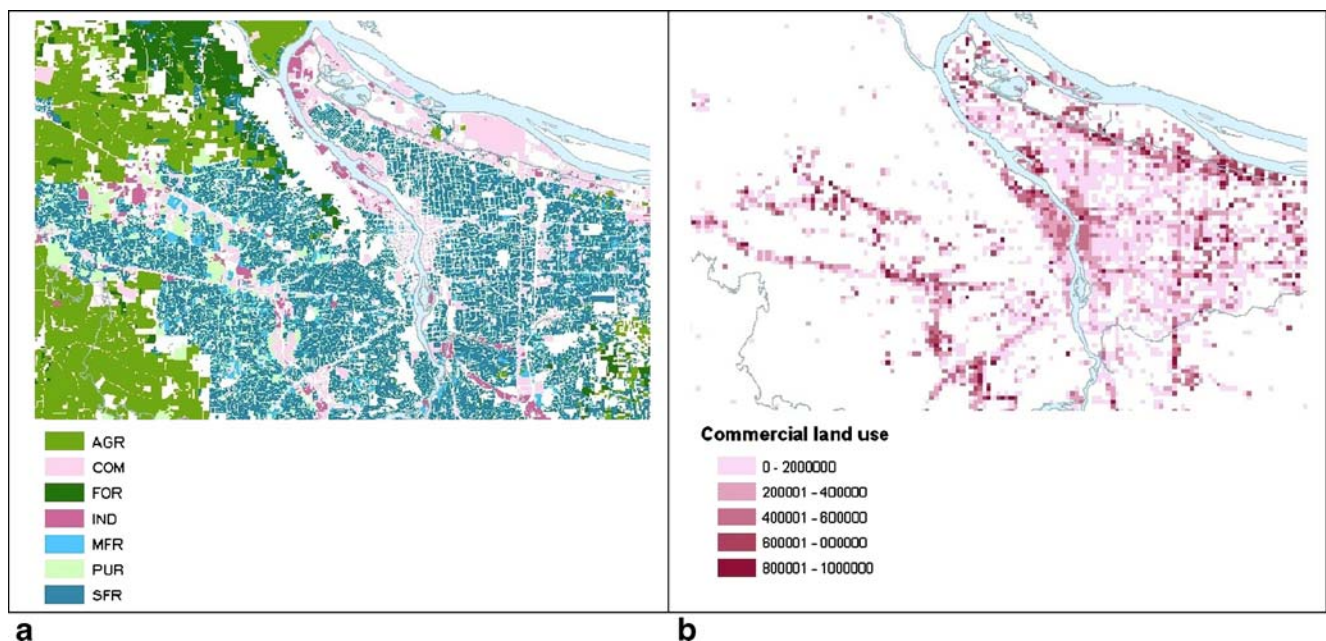


**Fig. 4** **a** Land-use in Portland (*AGR* agricultural, *COM* commercial, *FOR* forest, *IND* industrial, *MFR* multifamily residential, *PUB* public, *SFR* single family residential), **b** area of land-use that is commercial for each 300 m grid cell (units of area are in square feet)

mentioned above. A case (in this instance a grid cell) moves down a specific branch of the regression tree depending on if it satisfies the conditions of a rule, e.g. if one of the independent variables for that case is greater than or less than a particular value (Breiman et al. 1984). Once a case reaches a terminating node of the regression tree a multiple linear regression model for that node is used to predict the intensity of the UHI within that grid cell. This method allows for the determination of the most important land-use or surface variables affecting UHI intensity for different regions within the metropolitan area.

Raw land-use and surface variables were screened for multicollinearity, one of the assumptions of multiple regression analysis. Tolerance, which builds in the regression of each independent on all the others, was used to assess multivariate multicollinearity. Tolerance is  $1-R^2$  for the regression of an independent variable on all the other independents, ignoring the dependent, thus producing as many tolerance coefficients as there are independents. The higher the intercorrelation of the independents, the closer the tolerance approaches zero. As a rule of thumb, a tolerance less than 0.2 indicates a problem with multicollinearity and an increase in the standard error of the regression coefficients (Rawlings 1988).

### 2.8 Production of UHI intensity maps

Using the tree structured regression models it is possible to produce maps showing the spatial variability of UHI intensity across all areas of Portland where GIS information on land-use and surface cover are available.

## 3 Results

### 3.1 Vehicle temperature traverses

The spatial variability in temperatures measured across the urban area on the traverse day 26 June 2006 is presented in Fig. 5a. During the June 26th traverse, temperatures varied by 5.5°C across the area measured. The warmest temperatures experienced were close to the downtown area and in a region on the eastern side of the Willamette River. Coolest temperatures are in the region of Forest Park. Forest Park is a large forested park just west of downtown Portland that consists of over 20 km<sup>2</sup> of wooded area (Fig. 1). Figure 5b shows the spatial variability in the UHI intensity. Temperatures shown in this figure are the difference between the measured, elevation-corrected traverse temperature and the concurrent rural temperature. The UHI is shown to be positive in the downtown and the majority of the suburban areas, whilst there is a strong negative UHI (a cool island) in the area within and surrounding Forest Park.

### 3.2 Tree-structured regression

To examine any temporal differences in causality of UHI intensity, tree-structured regression models were produced separately for both weekend and weekday daytime UHI (of the six traverse days, three were on weekdays and three on weekends). Tolerance values for all variables in terminal-node multiple regression models were greater than 0.2, so there was no problem with multicollinearity between the independent variables.

The first rule for both the weekend and weekday daytime UHI regression trees differentiates between grid cells based on canopy cover (Fig. 6a,b). The first terminating node produces a predictive model for UHI intensity for areas where canopy cover is greater than 66% for the weekday traverses, and greater than 64% for the weekend traverses. This model predicts a negative UHI for those areas on the

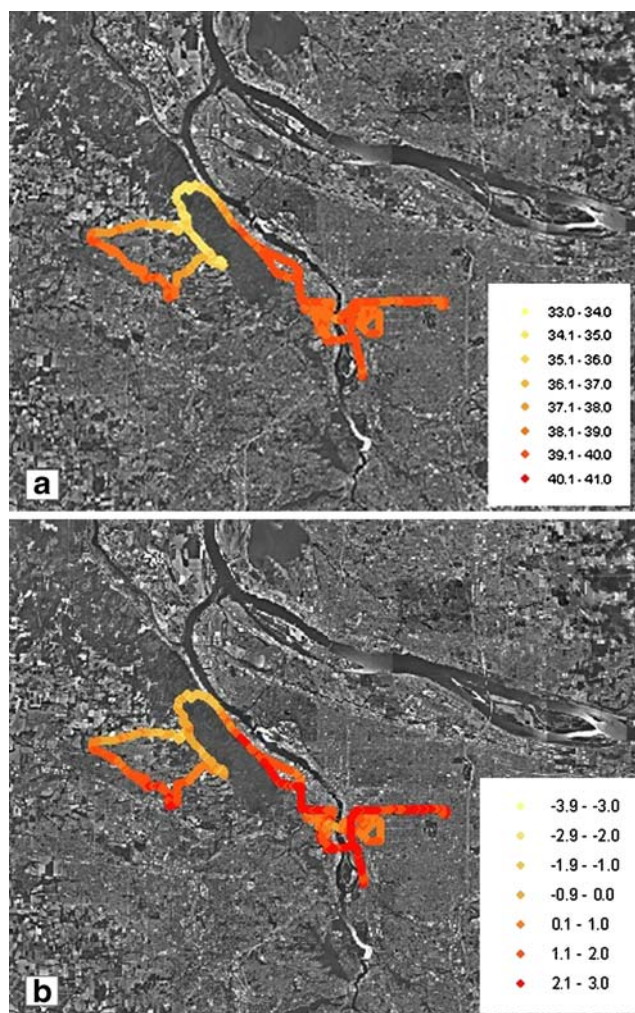


**Fig. 5** **a** Temperatures measured (the legend shows temperatures in degrees Celsius) and **b** UHI magnitude (the legend shows temperatures in degrees Celsius) during an afternoon vehicle traverse on 26 June 2006



order of  $-1.8^{\circ}\text{C}$  on for the weekdays and  $-2.6^{\circ}\text{C}$  for the weekend. Building floor space is the next most important determinant for both categories with a greater UHI intensity experienced in grid cells associated with less floor space. For the weekend model (Fig. 6a), building floor space is the last rule, for grid cells not satisfying rule 1 and occupying the first terminal node (therefore less canopy cover), highest temperatures were experienced when building floor space within the grid cell is less than  $19,113\text{ m}^2$ . The weekday model was further split by taking into account the total length of roads within a grid cell (Fig. 6b). For grid cells not satisfying rule 1 (canopy cover  $>66\%$ ) or rule 2 (total floor space  $>28,106\text{ m}^2$ ), rules 3 and 4 differentiate between the total length of roads within the grid cell with greater temperatures experienced when road lengths are less than  $1,161\text{ m}$  (mean UHI intensity of  $1.5^{\circ}\text{C}$ ).

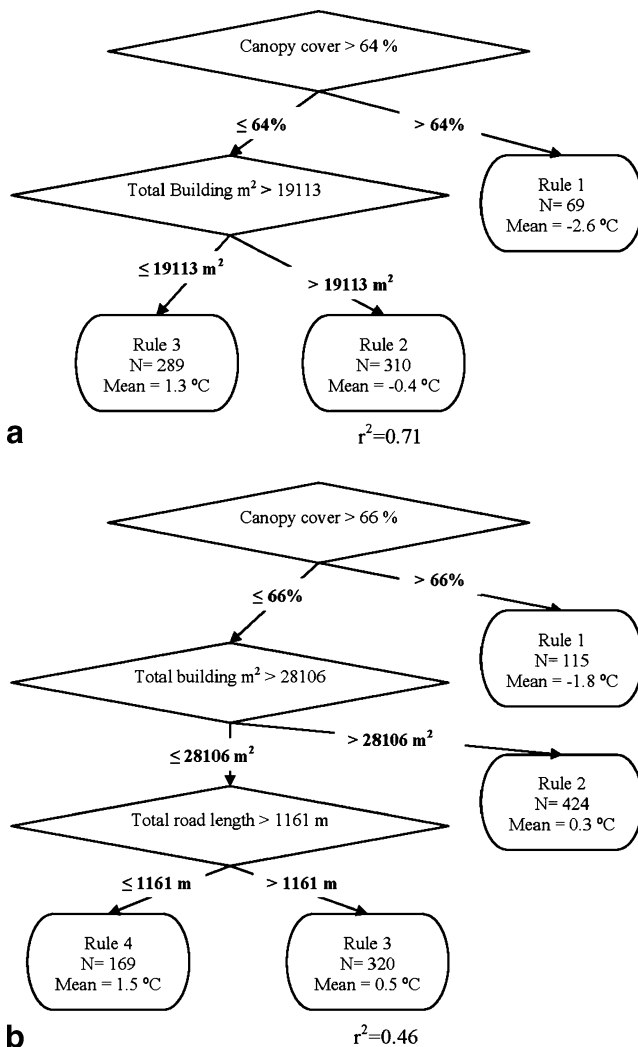


**Fig. 6** Tree-structured regression models for **a** weekend daytime UHI intensity, and **b** weekday daytime UHI intensity. *N* the number of grid cells within each terminating node; *Mean* the mean UHI intensity for that terminating node

### 3.3 UHI maps

Figure 7 presents the spatial variability of daytime (weekday and weekend) UHI intensity across the Portland metropolitan area, produced by applying the tree-structured regression models to the gridded land-use and surface characteristics. Accuracy of the predicted UHI intensity maps was determined by calculating the root mean square error (RMSE) between the grid average UHI intensity traverse observations and the grid UHI intensity calculated using the tree-structured regression models, this RSME was  $1.30^{\circ}\text{C}$  for the weekend map and  $2.30^{\circ}\text{C}$  for the weekday map.

Figure 7a,b illustrates that some regions within the Portland metropolitan area can experience a negative UHI during summertime afternoons. The regions that experience

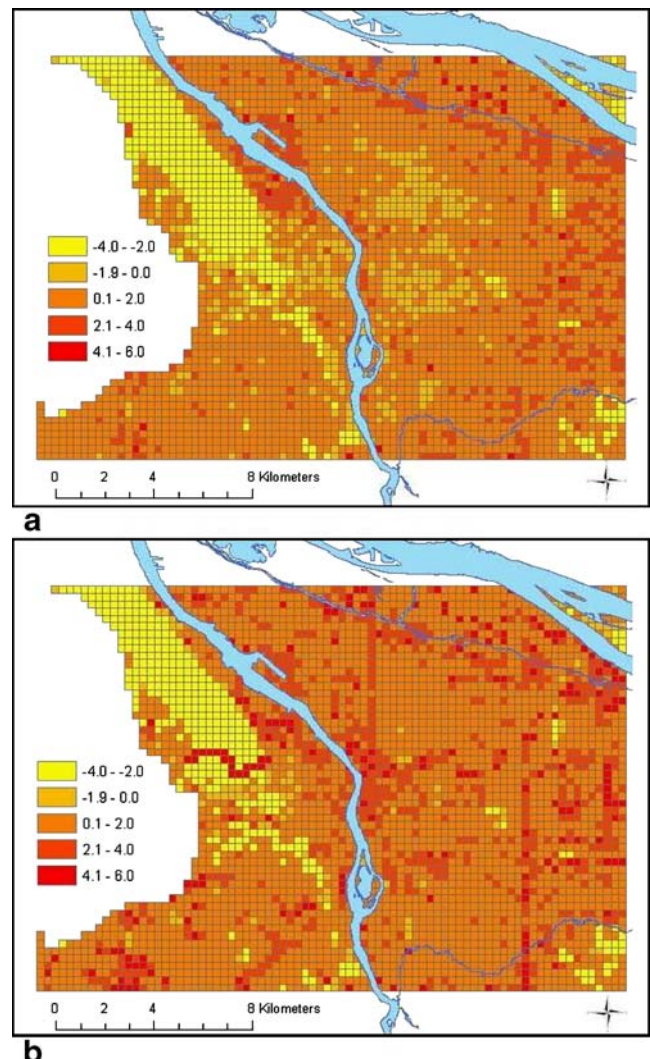


**Fig. 7** Grid values of UHI intensity produced using tree-structured regression models (UHI magnitude is in  $^{\circ}\text{C}$ ) for **a** weekend daytime UHI, and **b** weekday daytime UHI



a negative UHI are those with greatest canopy coverage as determined by the first rule of both the weekday and weekend daytime tree-structured regression models, this is generally the area encompassing Forest Park. Forest Park is the coolest region of the city on both weekdays and weekends and is generally 2–4°C cooler than the rural surroundings and can be up to 10°C cooler than surrounding urban regions. On weekend afternoons (Fig. 7a), the warmest temperatures are experienced in an industrial area to the north of the downtown. Some areas of downtown Portland and some pockets in the suburbs, particularly on the eastern side of the river, experience a small negative UHI during the weekend. On weekdays (Fig. 7b), the warmest areas of the city are just across the Willamette River (to the east) from the downtown area, an area characterised by commercial land-use, an industrial area just to the north of the downtown between Forest Park and the Willamette, and areas surrounding freeways and major roads, these regions experience a UHI intensity of up to 5°C. Downtown Portland, whilst experiencing a UHI of up to 2°C is not the warmest part of Portland on weekday summer afternoons. Suburban areas experience a UHI in the same magnitude as downtown.

#### 4 Discussion and conclusions

The most important urban characteristic separating warmer from cooler regions of the Portland metropolitan area was canopy cover, regardless of day of week. This illustrates the importance of parks and green spaces on the spatial variability of summertime urban air temperatures. Forest Park is unique in that it is a large (greater than 20 km<sup>2</sup>) park with extensive canopy cover surrounded by the Portland metropolitan area. The influence of Portland's Forest Park is greatest during the warmest part of the day when factors such as shading from the dense canopy and evapotranspiration are most important. This is consistent with investigations of the “park cool island” (PCI) effect by Spronken-Smith and Oke (1998) which found that parks with dense canopy cover have a maximum PCI in the afternoon, compared to garden and open grass parks which have a nocturnal maximum PCI.

Through the differentiation of weekday and weekend daytime intra-urban temperature differences, we are able to investigate the influence of anthropogenic activity on UHI intensity. The warmest area of the city regardless of time of day or week is a region associated with industrial land-use; the elevated temperatures experienced in this industrial region are probably due to a combination of lack of vegetation or canopy cover and continuous anthropogenic heat emissions. Anthropogenic heat emissions may also be a major factor in the elevated temperatures experienced in

commercial districts on weekday afternoons. Temperatures in these areas are up to 2°C cooler on weekend afternoons, often times when activity in commercial buildings is minimal.

Temperatures in the downtown core of Portland experience a 1–2°C stronger UHI intensity on weekday afternoons than weekend afternoons, once again this difference in UHI intensity can possibly be attributed to anthropogenic heat emissions, with emissions due to the building and transportation sector being less on weekends (Simmonds and Keay 1997; Shutters et al. 2006). The UHI intensity in the downtown core is smaller than some of the surrounding industrial and commercial areas, this is a phenomenon that has been documented in other cities and may be due to building canopy shading from the high rise buildings in the downtown core reducing the absorption of solar radiation during the day (Voogt 2002; Chow and Roth 2006).

The air masses near major arterial road surfaces are among the warmest of the city on weekdays, the impervious nature of roads reduces any likelihood of cooling through evapotranspiration; the low albedo and thermal properties of road surfaces absorb more solar radiation and emit more long-wave radiation. Temperatures along major roads during the daytime differ by up to 2°C on weekdays compared to weekends (Fig. 7a,b), with average UHI intensity for grid cells encompassing major arterial roads 1.9°C on weekdays and 0.6°C on weekends. This difference in UHI intensity is likely to be due to differences in anthropogenic activity on weekdays compared to weekends, particularly within the vehicle sector. Traffic density on weekends is less than on weekdays, daily vehicle miles travelled (DVMT) from the Oregon Department of Transportation (ODOT 2007) show that traffic density along major arterial roads in the Portland metropolitan area is 19% less on weekends compared to weekdays. This 19% difference in traffic density, along with weekday/weekend difference in anthropogenic heat release from the building sector, are likely explanations for the 1.3°C difference in UHI surrounding major arterial roads on weekdays compared to weekends.

This paper has introduced a method for investigating the spatial variability in UHI intensity using vehicle temperature traverses and GIS resources. Tree-structured regression models have allowed the determination of the most important land-use or surface variables affecting daytime summertime UHI intensity for different regions of a metropolitan area. The construction of separate models for weekday and weekend UHI has allowed for investigation of the influence of anthropogenic activity on UHI intensity on weekdays compared to weekends. Possibilities for extending the current analysis include: investigating the spatial variability of the UHI under different weather conditions, further investigation of temporal differences in UHI by undertaking vehicle

temperature traverses during additional times of the day, and expanding the analyses to also include winter months.

**Acknowledgements** The authors wish to thank the various participants in the traverse measurements. We also thank Kevin Martin, GIS specialist with the City of Portland Bureau of Planning for providing the GIS data. This research was supported by the National Science Foundation under Grant No. 0410103. Any opinions, findings, and conclusions or recommendations expressed in this material are those of the authors and do not necessarily reflect the views of the National Science Foundation.

## References

- Akbari H, Pomerantz M, Taha H (2001) Cool surfaces and shade trees to reduce energy use and improve air quality in urban areas. *Sol Energy* 70:295–310
- Arnfield J (2003) Two decades of urban climate research: a review of turbulence, exchanges of energy and water, and the urban heat island. *Int J Climatol* 23:1–26
- Arnfield J (2006) Micro- and mesoclimatology. *Prog Phys Geogr* 30
- Assimakopoulos MN, Mihalakakou G, Flocas HA (2007) Simulating the thermal behaviour of a building during summer period in the urban environment. *Renew Energy* 32(11):1805–1816
- Bornstein R, Lin Q (2000) Urban heat islands and summertime convective thunderstorms in Atlanta: three case studies. *Atmos Environ* 34:507–516
- Bottyan Z, Unger J (2003) A multiple linear statistical model for estimating the mean maximum urban heat island. *Theor Appl Climatol* 75:233–243
- Breiman L, Friedman JH, Stone CJ, Olshen RA (1984) Classification and regression trees. CRC, Boca Raton, FL, USA
- Changnon Jr SA, Huff FA, Semonin RG (1971) METROMEX: an investigation of inadvertent weather modification. *Bull Am Meteorol Soc* 52:958–968
- Chow WTL, Roth M (2006) Temporal dynamics of the urban heat island in Singapore. *Int J Climatol* 26:2243–2260. DOI 10.1002/joc.1364
- Chudnovsky A, Ben-Dor E, Saaroni H (2004) Diurnal thermal behavior of selected urban objects using remote sensing measurements. *Energy Build* 36:1063–1074
- City of Portland (2006) Natural resource inventory update: vegetation mapping project. City of Portland, Bureau of Planning, Portland, OR, 18 pp
- Erell E, Williamson T (2007) Intra-urban differences in canopy layer air temperature at a mid-latitude city. *Int J Climatol* 27(9):1243–1255
- George LA, Becker WB (2003) Investigating the urban heat island effect with a collaborative inquiry project. *J Geosci Educ* 51:237–243
- Giridharan R, Ganesan S, Lau SSY (2004) Daytime urban heat island effect in high-rise and high-density residential developments in Hong Kong. *Energy Build* 36:525–534. DOI 10.1016/j.enbuild.2003.12.016
- Giridharan R, Lau SSY, Ganesan S (2005) Nocturnal heat island effect in urban residential developments of Hong Kong. *Energy Build* 37:964–971. DOI 10.1016/j.enbuild.2004.12.005
- Giridharan R, Lau SSY, Ganesan S, Givoni B (2007) Urban design factors influencing heat island intensity in high-rise high-density environments of Hong Kong. *Build Environ* 42:3669–3684
- Huang H, Ooka R, Kato S (2005) Urban thermal environment measurements and numerical simulation for an actual complex urban area covering a large district heating and cooling system in summer. *Atmos Environ* 39:6362–6375. DOI 10.1016/j.atmosenv.2005.07.018
- Jauregui E, Romales E (1996) Urban effects on convective precipitation in Mexico City. *Atmos Environ* 30:3383–3389
- Jonsson P (2004) Vegetation as an urban climate control in the subtropical city of Gaborone, Botswana. *Int J Climatol* 24:1307–1322. DOI 10.1002/joc.1064
- Jusuf SK, Wong NH, Hagen E, Anggoro R, Hong Y (2007) The influence of land use on the urban heat island in Singapore. *Habitat Int* 31:232–242
- Kolokotroni M, Zhang Y, Watkins R (2007) The London heat island and building cooling design. *Sol Energy* 81:102–110. DOI 10.1016/j.solener.2006.06.005
- ODOT (2007) Daily vehicle miles traveled. ODOT, Salem, OR, Available Online. <http://www.oregon.gov/ODOT/>. Cited December 2007
- Portland Metro (2002) 2002–2022 urban growth report: a residential land need analysis. Portland Metro, Portland, OR, 42 pp
- Rawlins JO (1988) Applied regression analysis: a research tool. Wadsworth, Pacific Grove, CA, USA
- RLIS (2006) Regional land information system. Available Online. <http://www.metro-region.org/article.cfm?ArticleID=1024>. Cited June 2006
- Roth M (2002) Effects of cities on local climates. Workshop of IGES/APN Mega-City Project, Institute for Global Environmental Strategies, Kitakyushu, Japan, January 2002
- Rulequest (2006) Rulequest research data mining tools. Rulequest, St Ives, Australia, Available Online. <http://www.rulequest.com/>. Cited July 2006
- Saaroni H, Ben-Dor E, Bitan A, Potchter O (2000) Spatial distribution and microscale characteristics of the urban heat island in Tel-Aviv, Israel. *Landscape Urban Plan* 48:1–18
- Saitoh TS, Shimada T, Hoshi H (1996) Modeling and simulation of the Tokyo urban heat island. *Atmos Environ* 30:3431–3442
- Sailor DJ, Lu L (2004) A top-down methodology for developing diurnal and seasonal anthropogenic heating profiles for urban areas. *Atmos Environ* 38: 2737–2748
- Sarrat C, Lemonsu A, Masson V, Guedalia D (2006) Impact of urban heat island on regional atmospheric pollution. *Atmos Environ* 40:1743–1758. DOI 10.1016/j.atmosenv.2005.11.037
- Shutters ST, Balling J, Robert C (2006) Weekly periodicity of environmental variables in Phoenix, Arizona. *Atmos Environ* 40:304–310. DOI 10.1016/j.atmosenv.2005.09.037
- Simmonds I, Keay K (1997) Weekly cycle of meteorological variations in Melbourne and the role of pollution and anthropogenic heat release. *Atmos Environ* 31:1589–1603
- Souch C, Grimmond S (2006) Applied climatology: urban climate. *Prog Phys Geog* 30:270–279
- Spronken-Smith RA, Oke TR (1998) The thermal regime of urban parks in two cities with different summer climates. *Int J Remote Sens* 19:2085–2104
- Stone B, Norman JM (2006) Land use planning and surface heat island formation: a parcel-based radiation flux approach. *Atmos Environ* 40:3561–3573
- Taha H (1996) Modeling impacts of increased urban vegetation on ozone air quality in the south coast air basin. *Atmos Environ* 30:3423–3430
- Unger J (2004) Intra-urban relationships between surface geometry and urban heat island: review and new approach. *Climate Res* 27:253–264
- Unger J (2006) Modelling the annual mean maximum urban heat island using 2D and 3D surface parameters. *Climate Res* 30:215–226
- Voogt JA (2002) Urban heat island: causes and consequences of global environmental change, vol 2. Wiley, Chichester, NY, pp 660–666
- Wong NH, Yu C (2005) Study of green areas and urban heat island in a tropical city. *Habitat Int* 29:547–558